ОБЪЕДИНЕННЫЙ
ИНСТИТУТ
ЯДЕРНЫХ
ИССЛЕДОВАНИЙ

Дубна

E2-96-420

G.N.Afanasiev, S.M.Eliseev, Yu.P.Stepanovsky*

TRANSITION OF THE LIGHT VELOCITY BARRIER IN THE VAVILOV — ČERENKOV EFFECT

Submitted to «Proceedings of the Royal Society of London, series A»

*The Institute of Physics and Technology, Kharkov, Ukraine

1996

1 Introduction

Although the Vavilov-Čerenkov effect is a well established phenomenon widely used in physics and technology [1], many its aspects remain uninvestigated up to now. In particular, it is not clear how a transition takes place from the sublight velocity regime to the superlight one. Some time ago [2,3] it was suggested that alongside with the usual Čerenkov and bremsstrahlung shock waves, the shock wave associated with a charged particle overcoming the light velocity barrier should exist. The consideration presented there was pure qualitative without any formulae and numerical results. It was grounded on the analogy with phenomena occurring in acoustics and hydrodynamics. It seems to us that this analogy is not complete. In fact, the electromagnetic waves are pure transversal, while acoustic and hydrodynamic waves contain longitudinal components. Further, the analogy itself cannot be considered as a final proof. This fact and experimental ambiguity to distinguish the Čerenkov radiation from the bremsstrahlung one [4] make us consider effects arising from the charge particle overcoming the light barrier in the framework of the completely solvable model. To be more precise, we consider the straight-line motion of the point charge with a constant acceleration and evaluate the arising electromagnetic field (EMF). In accordance with refs. [2,3] we confirm the existence of the shock wave arising at the moment when charged particle overcomes the light velocity (inside the medium) barrier. This wave has essentially the same singularity as the Čerenkov shock wave. It is much stronger than the singularity of the bremsstrahlung shock wave.

Previously, the accelerated motion of the point charge in a vacuum was considered by Schott [5]. Yet, his qualitative consideration was pure geometrical, not allowing the numerical investigations.

The plan of our exposition is as follows. In sect. 2, the initial statement of the physical problem is given. The necessary mathematical details are presented in sect. 3. In particular, we solve the fourth-degree algebraic equation for the retardation times. The difficulty is not in solving the equation itself, but in the determination of space-time regions where the solutions exist. The physical analysis of the solutions obtained is given in sect. 4. In sect. 5, we consider a simplified case when the observation point lies on the axis of motion. The results of numerical calculations presented in sect. 6 and semi-analytic determination of the shock wave positions presented in sect. 7 seem to support the existence of the afore-mentioned shock waves suggested in [2,3]. A brief discussion and account of the results obtained are presented in sects. 8 and 9.

2 Statement of the physical problem

Let a charged particle move inside the medium with polarizabilities ϵ and μ along the given trajectory $\vec\xi(t)$. Then, its electromagnetic field (EMF) at the observation point (ρ, z) is given by the Lienard-Wiechert potentials

$$\Phi(\vec r,t)=\frac{e}{\epsilon}\sum\frac{1}{|R_i|},\quad \vec A(\vec r,t)=\frac{e\mu}{c}\sum\frac{\vec v_i}{|R_i|},\quad div\vec A+\frac{\epsilon\mu}{c}\dot\Phi=0 \tag{2.1}$$

Here

$$\vec v_i=\left(\frac{d\vec\xi}{dt}\right)\Big|_{t=t_i},\quad R_i=|\vec r-\vec\xi(t_i)|-\vec v_i(\vec r-\vec\xi(t_i))/c_n$$

and c_n is the light velocity inside the medium ($c_n=c/\sqrt{\epsilon\mu}$). Summation in (2.1) is performed over all physical roots of the equation

$$c_n(t-t')=|\vec r-\vec\xi(t')| \tag{2.2}$$

To preserve the causality, the time of radiation t' should be smaller than the observation time t'. Obviously, t' depends on the coordinates $\vec{r}, t$ of the point P at which the EMF is observed. With the account of (2.2) one gets for R_i

$$R_i = c_n(t - t_i) - \vec{v}_i(\vec{r} - \vec{\xi}(t_i)) \tag{2.3}$$

Consider the motion of the charged point-like particle moving inside the medium with a constant acceleration along the Z axis:

$$\xi = at^2 \tag{2.4}$$

The retarded times t' satisfy the following equation

$$c_n(t - t') = [\rho^2 + (z - at'^2)^2]^{1/2} \tag{2.5}$$

It is convenient to introduce the dimensionless variables

$$\tilde{t} = at/c_n, \quad \tilde{z} = az/c_n^2, \quad \tilde{\rho} = a\rho/c_n^2 \tag{2.6}$$

Then,

$$\tilde{t} - \tilde{t}' = [\tilde{\rho}^2 + (\tilde{z} - \tilde{t}'^2)^2]^{1/2} \tag{2.7}$$

In order not to overload exposition, we drop the tilda signs:

$$t - t' = [\rho^2 + (z - t'^2)^2]^{1/2} \tag{2.8}$$

For the treated case of one-dimensional motion the denominators R_i are given by:

$$R_i = \frac{c_n^2}{a} r_i, \quad r_i = (t - t_i) - 2t_i(z - t_i^2) \tag{2.9}$$

We consider the following two problems :

I. A charged particle rests at the origin up to a moment $t = 0$. After that it is uniformly accelerated in the positive direction of the Z axis. In this case only positive retarded times t' have a physical meaning.

II. A charged particle decelerates uniformly moving from $z = \infty$ to the origin. After the moment $t = 0$ it rests there. Only negative retarded times are physical in this case.

It is our aim to investigate space-time distribution of the EMF arising from such particle motions.

3 Mathematical preliminaries

Eq.(2.8) is reduced to the following equation of fourth degree

$$t'^4 + pt'^2 + qt' + R = 0 \tag{3.1}$$

Here $p = -2(z + 1/2)$, $q = 2t$, $R = r^2 - t^2$. To find the roots of (3.1), it is preliminary needed to solve the following equation of the third degree [6]:

$$\Theta^3 - 2p\Theta^2 + (p^2 - 4R)\Theta + q^2 = 0 \tag{3.2}$$

The substitution $\Theta = \Theta_1 + \frac{2}{3}p$ reduces (3.2) to the canonical form

$$\Theta_c^3 + p_1\Theta_c + q_1 = 0 \tag{3.3}$$

Here $p_1 = -\frac{1}{3}p^2 - 4R$, $q_1 = \frac{2}{27}p^3 - \frac{8}{3}pR + 4t^2$. The solutions of Eq.(3.2) are determined by its discriminant

$$D_1 = -4p_1^3 - 27q_1^2 \tag{3.4}$$

In what follows we need the following three representations of D_1:

$$-\frac{D_1}{256} = t^6 - t^4(3\rho^2 + z^2 + \frac{5}{2}z + \frac{1}{16}) + t^2[3\rho^4 + 2z(z^2 + z + \frac{1}{16}) + 2\rho^2 z^2 + \frac{1}{2}\rho^2 z + \frac{5}{4}\rho^2] -$$
$$-r^2(\rho^2 - z - \frac{1}{4})^2 \tag{3.5}$$

$$\frac{D_1}{256} = \rho^6 + \rho^4[z^2 - 2(z + \frac{1}{4}) - 3t^2] + \rho^2[(z + \frac{1}{4})^2 - 2z^2(z + \frac{1}{4}) + 3t^4 - t^2(2z^2 + \frac{z}{2} + \frac{5}{4})] -$$
$$-[t^2 - (z + \frac{1}{4})^2](t^2 - z)^2 \tag{3.6}$$

$$\frac{D_1}{256} = \frac{1}{16}p^4 R - \frac{1}{64}p^3 q^2 - \frac{1}{2}p^2 R^2 + \frac{9}{16}pq^2 R - \frac{27}{256}q^4 + R^3 \tag{3.7}$$

Then it follows that $D_1 > 0$ for $\rho \to \infty$ and z, t fixed; $D_1 > 0$ for $|z| \to \infty$ and ρ, t fixed; $D_1 < 0$ for $t \to \infty$ and ρ, z fixed. The solution of (3.2) has the form

$$\Theta_1 = \frac{2p}{3} + \frac{1}{3}[(\rho, x_1) + (\rho^2, x_1)],$$

$$\Theta_2 = \frac{2p}{3} - \frac{1}{6}[(\rho, x_1) + (\rho^2, x_1)] - \frac{i}{2\sqrt{3}}[(\rho, x_1) - (\rho^2, x_1)],$$

$$\Theta_3 = \frac{2p}{3} - \frac{1}{6}[(\rho, x_1) + (\rho^2, x_1)] + \frac{i}{2\sqrt{3}}[(\rho, x_1) - (\rho^2, x_1)] \tag{3.8}$$

Here

$$(\rho, x_1) = (-\frac{27}{2}q_1 + \frac{3}{2}\sqrt{-3D_1})^{1/3}, \quad (\rho^2, x_1) = (-\frac{27}{2}q_1 - \frac{3}{2}\sqrt{-3D_1})^{1/3}$$

(the notation Θ_i, (ρ, x_1) and (ρ^2, x_1) is taken from the Van der Waerden treatise [6]). The following equalities should be satisfied

$$(\rho, x_1)(\rho^2, x_1) = -3p_1, \quad \Theta_1\Theta_2\Theta_3 = -4t^2$$

As $\Theta_2 \cdot \Theta_3 > 0$, it should be

$$\Theta_1 = \frac{2}{3}p + \frac{1}{3}[(\rho, x_1) + (\rho^2, x_1)] < 0 \tag{3.9}$$

The roots of (3.1) are expressed through Θ_i:

$$t_1 = \frac{1}{2}(\sqrt{-\Theta_1} + \sqrt{-\Theta_2} + \sqrt{-\Theta_3}), \quad t_2 = \frac{1}{2}(\sqrt{-\Theta_1} - \sqrt{-\Theta_2} - \sqrt{-\Theta_3}),$$

$$t_3 = \frac{1}{2}(\sqrt{-\Theta_2} - \sqrt{-\Theta_1} - \sqrt{-\Theta_3}), \quad t_4 = \frac{1}{2}(\sqrt{-\Theta_3} - \sqrt{-\Theta_1} - \sqrt{-\Theta_2}) \tag{3.10}$$

The following condition should also be satisfied:

$$\sqrt{-\Theta_1}\sqrt{-\Theta_2}\sqrt{-\Theta_3} = -2t \tag{3.11}$$

If we choose $\sqrt{-\Theta_3}\cdot\sqrt{-\Theta_2} > 0$, then $\sqrt{-\Theta_1}$ should be negative for $t > 0$ and positive for $t < 0$. The retarded times t_i have different forms for $D_1 > 0$ and $D_1 > 0$. For $D_1 < 0$:

$$t_1 = -\frac{t}{\sqrt{a^2+b^2}} + \frac{1}{\sqrt{2}}[a+\sqrt{(a^2+b^2)}]^{1/2}, \quad t_2 = -\frac{t}{\sqrt{a^2+b^2}} - \frac{1}{\sqrt{2}}[a+\sqrt{(a^2+b^2)}]^{1/2},$$

$$t_3 = \frac{t}{\sqrt{a^2+b^2}} + \frac{i}{\sqrt{2}}[a+\sqrt{(a^2+b^2)}]^{1/2}, \quad t_4 = \frac{t}{\sqrt{a^2+b^2}}t - \frac{i}{\sqrt{2}}[a+\sqrt{(a^2+b^2)}]^{1/2} \tag{3.12}$$

Here

$$a = \frac{4}{3}(z+\frac{1}{2}) + \frac{1}{6}[(\rho,z_1)+(\rho^2,z_1)], \quad b = \frac{1}{2\sqrt{3}}[(\rho,z_1)-(\rho^2,z_1)].$$

t_3 and t_4 in (3.12) contain imaginary parts and, therefore, are not admissible.
For $D_1 > 0$ (only $p_1 < 0$ is possible in this case) there are two different cases corresponding to $q_1 > 0$ and $q_1 < 0$.
For $q_1 > 0$ one has:

$$\Theta_1 = \frac{2}{3}p - \frac{2}{3}\sqrt{-3p_1}\cos\frac{\phi_1}{3}, \quad \Theta_2 = \frac{2}{3}p + \frac{1}{3}\sqrt{-3p_1}\cos\frac{\phi_1}{3} + \frac{1}{\sqrt{3}}\sqrt{-3p_1}\sin\frac{\phi_1}{3},$$

$$\Theta_3 = \frac{2}{3}p + \frac{1}{3}\sqrt{-3p_1}\cos\frac{\phi_1}{3} - \frac{1}{\sqrt{3}}\sqrt{-3p_1}\sin\frac{\phi_1}{3} \tag{3.13}$$

Here $\cos\phi_1 = \frac{27}{2}|q_1|/\sqrt{-27p_1^3}$, $\sin\phi_1 = \frac{3}{2}\sqrt{3D_1}/\sqrt{-27p_1^3}$, $0 \le \varphi_1 \le \pi/2$.
It is easy to check that $\Theta_2 > \Theta_3 > \Theta_1$. Further, $\Theta_2 > 0$ and $\Theta_3 > 0$ for $p > 0$. As t_i are obtained by extracting square roots of $-\Theta_i$, all t_i in (3.10) contain imaginary parts, which is not physically permissible. For $p < 0$ one has $\Theta_1 < 0$, while both Θ_2 and Θ_3 are negative if

$$\frac{2}{3}|p| - \frac{1}{3}\sqrt{-3p_1}\cos\frac{\phi_1}{3} - \frac{1}{\sqrt{3}}\sqrt{-3p_1}\sin\frac{\phi_1}{3} > 0 \tag{3.14}$$

Thus, a physical solution for $D_1 > 0$, $q_1 > 0$ is possible only if $p < 0$, which corresponds to $z > -1/2$.
For $q_1 < 0$ one has:

$$\Theta_1 = \frac{2}{3}p + \frac{2}{3}\sqrt{-3p_1}\cos\frac{\phi_1}{3}, \quad \Theta_2 = \frac{2}{3}p - \frac{1}{3}\sqrt{-3p_1}\cos\frac{\phi_1}{3} + \frac{1}{\sqrt{3}}\sqrt{-3p_1}\sin\frac{\phi_1}{3},$$

$$\Theta_3 = \frac{2}{3}p - \frac{1}{3}\sqrt{-3p_1}\cos\frac{\phi_1}{3} - \frac{1}{\sqrt{3}}\sqrt{-3p_1}\sin\frac{\phi_1}{3} \tag{3.15}$$

In this case $\Theta_1 > \Theta_2 > \Theta_3$. Further, $\Theta_1 > 0$ for $p > 0$. This leads to the appearance of imaginary parts in all Θ_i, which is not allowable. It turns out that $\Theta_2 < 0, \Theta_3 < 0$ for $p < 0$, while Θ_1 is negative if

$$\frac{2}{3}|p| - \frac{2}{3}\sqrt{-3p_1}\cos\frac{\phi_1}{3} > 0 \tag{3.16}$$

We conclude: the physical solution can appear for $D_1 > 0$ in those space-time regions for which conditions $z > -1/2$, (3.14) and (3.16) are fulfilled.
To distinguish the space-time regions where $D_1 > 0$ from those where $D_1 < 0$, one should find the roots of equation $D_1 = 0$. For this we present D_1 in the form:

$$D_1 = [\rho^2 - \rho_1(t,z)][\rho^2 - \rho_2(t,z)][\rho^2 - \rho_3(t,z)] \tag{3.17}$$

For (t, z) fixed the roots ρ_i define the space regions in which D_1 as a function of ρ changes its sign. To find ρ_i, one should find the discriminant D_2 of the equation $D_1 = 0$ with D_1 taken in the form (3.6). It equals

$$D_2 = -16t^2[\frac{27}{16}t^2 - (z+1/2)^3]^3 \tag{3.18}$$

Obviously, $D_2 < 0$ for $z < z_c$ and $D_2 > 0$ for $z > z_c$. Here $z_c = -\frac{1}{2} + 3(\frac{t}{4})^{2/3}$. For $z < z_c$ the equation $D_1 = 0$ has only one real root, while three real roots are possible for $z > z_c$. For $z < z_c$ one gets:

$$\frac{D_1}{256} = (\rho^2 + \delta - \rho_1)|F|^2, \quad \rho_1 = \frac{1}{3}[(\rho,z_2)+(\rho^2,z_2)], \quad (\rho,z_2) = (\frac{3}{2}\sqrt{-3D_2} - \frac{27}{2}q_2)^{1/3},$$

$$(\rho^2,z_2) = (-\frac{3}{2}\sqrt{-3D_2} - \frac{27}{2}q_2)^{1/3}, \quad q_2 = -\frac{27}{16}t^4 - \frac{5}{2}t^2(z+\frac{1}{2})^3 + \frac{2}{27}(z+\frac{1}{2})^6,$$

$$|F|^2 = [\rho^2+\delta+\frac{1}{6}((\rho,z_2)+(\rho^2,z_2))]^2 + \frac{1}{12}[(\rho,z_2)-(\rho^2,z_2)]^2, \quad \delta = \frac{1}{3}[z^2 - 2(z+\frac{1}{4}) - 3t^2] \tag{3.19}$$

For $z > z_c$ one gets

$$\frac{D_1}{256} = (\rho^2 + \delta - \rho_2)(\rho^2 + \delta - \rho_3)(\rho^2 + \delta - \rho_4) \tag{3.20}$$

Here

$$\rho_2 = \pm\frac{2}{3}\sqrt{-3p_2}\cos\frac{\phi_2}{3}, \quad \rho_3 = \mp\frac{1}{3}\sqrt{-3p_2}\cos\frac{\phi_2}{3} + \sqrt{-p_2}\sin\frac{\phi_2}{3},$$

$$\rho_4 = \mp\frac{1}{3}\sqrt{-3p_2}\cos\frac{\phi_2}{3} - \sqrt{-p_2}\sin\frac{\phi_2}{3}$$

(the upper and lower signs correspond to $q_2 < 0$ and $q_2 > 0$, resp.) Further,

$$p_2 = -\frac{9}{2}(z+\frac{1}{2})t^2 - \frac{1}{3}(z+\frac{1}{2})^4, \quad \cos\phi_2 = \frac{27}{2}\frac{|q_2|}{\sqrt{-27p_2^3}}, \quad \sin\phi_2 = \frac{3}{2}\frac{\sqrt{3D_2}}{\sqrt{-27p_2^3}}$$

4 Elaboration of the physical problem

Accelerated motion.
In this case the retarded times t_i and the observation time t should be positive. As $t_2 < 0$ in (3.12), it is physically inadmissible. Thus, for the region where $D_1 < 0$ only t_1 root survives under the condition that $0 < t_1 < t$.
Now we turn to the case $D_1 > 0, q_1 > 0$. The $\sqrt{-\Theta_i}$ entering into (3.10) are

$$\sqrt{-\Theta_1} = -(\frac{2}{3}|p| + \frac{2}{3}\sqrt{-3p_1}\cos\frac{\phi_1}{3})^{1/2}, \quad \sqrt{-\Theta_2} = (\frac{2}{3}|p| - \frac{1}{3}\sqrt{-3p_1}\cos\frac{\phi_1}{3} - \sqrt{-p_1}\sin\frac{\phi_1}{3})^{1/2}$$

$$\sqrt{-\Theta_3} = (\frac{2}{3}|p| - \frac{1}{3}\sqrt{-3p_1}\cos\frac{\phi_1}{3} + \sqrt{-p_1}\sin\frac{\phi_1}{3})^{1/2} \tag{4.1}$$

In what follows we enumerate the roots (3.10) corresponding to $D_1 > 0$ as t_3, t_4, t_5, t_6. Substituting (4.1) into (3.10) we see that

$$t_6 > t_5 > t_3 > t_4, \quad t_4 < 0, \quad t_5 > 0, \quad t_6 > 0 \tag{4.2}$$

while the sign of t_3 may be different in different space-time regions. As $t_4 < 0$ it should be discarded. Then, equations

$$0 < t_3 < t, \quad t_5 < t, \quad t_6 < t \tag{4.3}$$

combined with (3.14) define the space-time regions where the particular solution $t_i (i = 3, ..., 6)$ exists.
The similar equations for $D_1 > 0, \quad q_1 < 0$ are:

$$\sqrt{-\Theta_1} = -(\frac{2}{3}|p| - \frac{2}{3}\sqrt{-3p_1}\cos\frac{\phi_1}{3})^{1/2}, \quad \sqrt{-\Theta_2} = (\frac{2}{3}|p| + \frac{1}{3}\sqrt{-3p_1}\cos\frac{\phi_1}{3} - \sqrt{-p_1}\sin\frac{\phi_1}{3})^{1/2},$$

$$\sqrt{-\Theta_3} = (\frac{2}{3}|p| + \frac{1}{3}\sqrt{-3p_1}\cos\frac{\phi_1}{3} + \sqrt{-p_1}\sin\frac{\phi_1}{3})^{1/2} \qquad (4.4)$$

One gets from (3.10) that

$$t_3 > t_6 > t_5 > t_4, \quad t_3 > 0, \quad t_4 < 0, \quad t_6 > 0 \qquad (4.5)$$

while the sign of t_5 varies from one point to another. Again, the retarded solution t_4 is not physically admissible. Thus, the conditions

$$t_3 < t, \quad t_6 < t, \quad 0 < t_5 < t \qquad (4.6)$$

combined with (3.16) define the space-time region where the particular solution exists.

Decelerated motion.

2) The second problem deals with the charged particle which decelerates uniformly. The charge equation of motion is still given by (2.1), but the retarded times t_i should be negative now. We consider the positive and negative observation times separately.
For $t > 0, D_1 < 0$ the retarded time t_2 is negative, while the sign of t_1 changes from point to point. Thus, solution t_2 exists everywhere, while t_1 exists in those regions which meet the condition $t_1 < 0$.
It turns out that for $D_1 > 0, \quad q_1 > 0$ Eqs. (4.2) are still valid. As retarded times t_5 and t_6 are positive, they should be discarded. Further, the retarded solution t_4 exists in the space regions where Eq.(3.14) is satisfied, while t_3 exists in the regions where Eqs.(3.14) and $t_3 < 0$ are fulfilled.
For $D_1 > 0, \quad q_1 < 0$ Eqs.(4.5) are valid. The positivity of t_3 and t_6 implies that they should be discarded. The retarded solutions t_4 and t_5 exist in those space-time regions where Eqs. (3.16) (for t_4) and (3.16) and $t_5 < 0$ (for t_5) are fulfilled.
For $t < 0$ the retarded time $t_1 > 0$ that is not physically acceptable. On the other hand, t_2 contributes to those space-time-regions which meet conditions (3.9) and $t_2 < t$.
For $t < 0, \quad D_1 > 0, \quad q_1 > 0$ the $\sqrt{-\Theta_i}$ entering into (3.10) are given by

$$\sqrt{-\Theta_1} = (\frac{2}{3}|p| + \frac{2}{3}\sqrt{-3p_1}\cos\frac{\phi_1}{3})^{1/2}, \quad \sqrt{-\Theta_2} = (\frac{2}{3}|p| - \frac{1}{3}\sqrt{-3p_1}\cos\frac{\phi_1}{3} - \sqrt{-p_1}\sin\frac{\phi_1}{3})^{1/2}$$

$$\sqrt{-\Theta_3} = (\frac{2}{3}|p| - \frac{1}{3}\sqrt{-3p_1}\cos\frac{\phi_1}{3} + \sqrt{-p_1}\sin\frac{\phi_1}{3})^{1/2} \qquad (4.7)$$

Further, $t_3 > t_4 > t_6 > t_5$. It turns out that $t_3 > 0, \quad t_5 < 0, \quad t_6 < 0$ while the sign of t_4 changes from point to point. Thus, conditions for existence of these retarded solutions are

$$t_5 < t, \quad t_6 < t, \quad t_4 < t \qquad (4.8)$$

These conditions should be supplemented by Eq.(3.14).
For $D_1 > 0, q_1 < 0$ one gets: $t_3 > t_6 > t_5 > t_4$,

$$\sqrt{-\Theta_1} = (\frac{2}{3}|p| - \frac{2}{3}\sqrt{-3p_1}\cos\frac{\phi_1}{3})^{1/2}, \quad \sqrt{-\Theta_2} = (\frac{2}{3}|p| + \frac{1}{3}\sqrt{-3p_1}\cos\frac{\phi_1}{3} - \sqrt{-p_1}\sin\frac{\phi_1}{3})^{1/2},$$

$$\sqrt{-\Theta_3} = (\frac{2}{3}|p| + \frac{1}{3}\sqrt{-3p_1}\cos\frac{\phi_1}{3} + \sqrt{-p_1}\sin\frac{\phi_1}{3})^{1/2} \qquad (4.9)$$

Now $t_3 > 0, \quad t_4 < 0, \quad t_5 < 0$ while the sign of t_6 may vary. The conditions for the existence of these retarded solutions are (3.16) and

$$t_4 < t, \quad t_5 < t, \quad t_6 < t \qquad (4.10)$$

5 Particular case

Before going to the numerical calculations it is instructive to consider a simple case corresponding to the observation point lying on the Z axis ($\rho = 0$). In this case

$$-\frac{D_1}{256} = [t^2 - (z + \frac{1}{4})^2](t^2 - z)^2 \qquad (5.1)$$

The roots of Eq.(3.1) are given by

$$t_1 = \tau_1 - 1/2, \quad t_2 = \tau_2 + 1/2, \quad t_3 = -\tau_2 + 1/2, \quad t_4 = -\tau_1 - 1/2, \qquad (5.2)$$

$$\tau_1 = \sqrt{z + t + 1/4}, \quad \tau_2 = \sqrt{z - t + 1/4}$$

In what follows we need also the values of denominators R_i entering into the definition of electromagnetic potentials $\Phi, \vec{A}$:

$$r_1 = 2\tau_1(t + 1/2 - \tau_1), \quad r_2 = 2\tau_2(-t + 1/2 + \tau_2),$$

$$r_3 = 2\tau_2(t - 1/2 + \tau_2), \quad r_4 = -2\tau_1(t + 1/2 + \tau_1) \qquad (5.3)$$

Accelerated motion.

For the first problem (uniform acceleration of the charged particle from the state of rest) the physical retarded times are (fig.1):

i) t_1.

This solution exists in the space-time region $-t < z < t^2$. It consists of three subregions. Subregion $t > 1/8, \quad -t < z < t - 1/4$ corresponds to $D_1 < 0$, while subregions $t < 1/8, \quad -t < z < t^2$ and $t > 1/8, \quad t - 1/4 < z < t^2$ correspond to $D_1 > 0$.

ii) t_2.

This solution exists in the $t > 1/2, \quad t - 1/4 < z < t^2$ region and corresponds to $D_1 > 0$.

iii) t_3.

This solution exists in the regions $t < 1/2, \quad t^2 < z < t$ and $t > 1/2, \quad t - 1/4 < z < t$ and corresponds to $D_1 > 0$.

Let the observer be placed at a particular point of the Z axis. We clarify now what he will see at different moments of time. It is convenient to relate the current time t not to the retarded time t_r, but to the particle position z_r at that moment of time ($z_r = t_r^2$).

Consider the particular point P lying on the negative Z semi-axis (fig.2). Up to the moment $t = -z$ the observer sees the field of the charge resting at the origin. At the moment $t = -z$ the shock wave arising from the beginning of the particle motion arrives at P. At later times the radiation arrives from the retarded particle positions z_1 lying to the right of P.

Let the observation point P lie on the positive Z semi-axis in the interval $0 < z < 1/4$ (fig.3). Up to a moment $t = z$ the observer in P sees the electrostatic field of the charge resting at the origin. At the moment $t = z$ the bremsstrahlung shock wave from the origin reaches P. In the time interval $z < t < \sqrt{t}$ the retarded solution is t_3 which describes the radiation from the particle retarded positions lying in the interval $0 < z_r < z$. At the moment $t = \sqrt{z}$ the charged particle reaches the observation point P. At that point R_1 and R_3 defined by Eq.(5.3) vanish and the electromagnetic potentials are infinite. For time $t > \sqrt{z}$ the observer detects the radiation from the retarded positions of the particle lying at the right of P and corresponding to t_1.

Let the observation point lie in the interval $1/4 < z < 1$ (fig.4). Up to a moment $t = z$ the observer sees the field of the charge at rest. At the moment $t = z$ the bremsstrahlung shock wave originating from the beginning of the charge motion reaches P. In the time interval $z < t < \sqrt{z}$ the observer sees the radiation from the particle retarded positions (z_3) in the interval $0 < z_r < (1 - \sqrt{z})^2$. At the moment $t = \sqrt{z}$ the charged particle (or Čerenkov shock wave) reaches the observation point. Again, electromagnetic potentials are infinite at this point. After that ($\sqrt{z} < t < z + 1/4$) the observer in P detects the radiation from three retarded positions of the particle. Two of them (z_2 and z_3) lie to the left of the observation point P and on the opposite sides of the point $z_l = 1/4$ at which the particle velocity is equal to the light velocity in the medium. As time goes, these retarded radiation points approach z_l. At the moment $t = z + 1/4$ they fuse at the point $z_l = 1/4$ where particle velocity equals to c_n. It turns out (see (5.3)) that at this point R_2 and R_3 vanish while the electromagnetic potentials take the infinite values. The disappearance of the t_2 and t_3 solutions and the infinite values of electromagnetic potentials suggests that the observation point is reached by the shock wave originating from the point $z_l = 1/4$ where the particle velocity was equal to c_n. The third of the mentioned solutions (t_1) describes the radiation from the particle positions lying to the right of the observation point. For $t > z + 1/4$ only this solution contributes to the observation point.

Let the observation point P lie in the region $z > 1$ (fig.5). Up to a moment $t = \sqrt{z}$ the observer sees the electrostatic field of the charge in rest. At the moment $t = \sqrt{z}$ the charged particle (with the Mach cone accompanying it) arrives at P. The electromagnetic potentials are infinite at this moment. In the time interval $\sqrt{z} < t < z$ the observer detects the electrostatic field of the charge in rest and the radiation from two points lying to the left (z_2) and the right (z_1) of P. At the moment $t = z$ the bremsstrahlung shock wave from the origin reaches P. In the time interval $z < t < z + 1/4$ there are three retarded solutions ($t_1; t_2, t_3$) which contribute to P. At the moment $t = z + 1/4$ the retarded solutions t_2 and t_3 annihiliate each other at the point $z_l = 1/4$ where the particle velocity is equal to c_n. This, as well as infinite values of the electromagnetic potentials, imply the existence of the shock wave originating from $z_l = 1/4$. For $t > z + 1/4$ only the radiation from t_1 solution reaches P.

Decelerated motion.

In the second case (uniform deceleration of the charge up to a moment $t = 0$ after which it rests at the origin) the allowable retarded solutions are (fig.6):

i) t_4.

This solution exists in the regions $t < -1/2, \quad z > t^2$ and $t > -1/2, \quad z > -t - 1/4$. In the first of them $D_1 > 0$; the second region contains two subregions $-1/2 < t < 0, \quad z > -t - 1/4$ and $t > 0, \quad z > t - 1/4$ corresponding to $D_1 > 0$ and one subregion $t > 0, \quad -t - 1/4 < z < t - 1/4$ corresponding to $D_1 < 0$.

ii) t_3.

This solution exists in regions $t < 0, \quad z > t^2$ and $t > 0, \quad z > t$ and corresponds to $D_1 > 0$.

iii) t_1.

This solution is defined in the region $-1/2 < t < 0, \quad -t - 1/4 < z < t^2$ where $D_1 > 0$ and in the region $t > 0, \quad -t - 1/4 < z < -t$ where $D_1 < 0$.

Let the observer be placed on the negative Z semi-axis (fig.7). Up to a moment $t = -z - 1/4$ he does not obtain any information concerning the particle motion. At the moment $t = -z - 1/4$ the shock wave originating from the particle overcoming the light velocity barrier (at $z_l = 1/4, \quad t_l = -1/2$)) reaches the observation point P (the electromagnetic potentials are infinite at this point). In the time interval $-z - 1/4 < t < -z$ the observer detects the radiation from two retarded charge positions lying to the left (z_1) and right (z_4) of z_l. At the moment $t = -z$ the observer detects the shock wave arising from the termination of the particle motion. For $t > -z$ the observer sees the electrostatic field of the charge which rests at the origin and the radiation from the remote retarded positions z_4 of the charge.

Let the observation point lie within the interval $0 < z < 1/4$ (fig.8). At the moment $t = -z - 1/4$ the shock wave originating from the particle overcoming the light velocity barrier (at $z = z_l$) reaches the observer. Again, the electromagnetic potentials are infinite at this moment. In the time interval $-z - 1/4 < t < -\sqrt{z}$ the radiations from two retarded positions of the charge (z_4 and z_1) arrive to P. They lie on different sides of z_l, to the right of the observation point z. As time goes, one of the radiating points (z_1) approaches the origin, while the other (z_4) moves away from z. At the moment $t = -\sqrt{z}$ the electromagnetic potentials become infinite as the charged particle arrives at P. At this moment the t_1 solution disappears, but, instead, t_3 arises. In the time interval $-\sqrt{z} < t < z$ the observer sees the radiation from two points lying on different sides of him. At the moment $t = z$ one of the retarded positions of the charge (z_3) comes to the origin and the corresponding bremsstrahlung shock wave reaches the observer. For times $t > z$ the observer sees the electrostatic field of the charge at rest and the radiation field from the remote retarded positions z_4 of the charge.

Let the observer be placed at the point P with $z > 1/4$ (fig.9). There is no field in P up to a moment $t = \sqrt{z}$. At this moment the charge arrives at P. After that the observer sees the radiation field from two retarded positions lying on different sides of P. As time goes, one of the retarded positions (z_3) approaches the origin, while the other (z_4) goes away. At the moment $t = z$ the observer sees that charge reaches the origin and detects the shock wave associated with the termination of the particle motion. After that moment the observer detects the electrostatic field of the charge which rests at the origin and the radiation field from one remote retarded position of the charge.

Concluding this section we note the existence of two types of the shock waves. The bremsstrahlung shock waves associated with the beginning or termination of the charge motion correspond to finite jumps of electromagnetic potentials. Therefore, the field strengths have the δ-type singularities. On the other hand, the Čerenkov shock wave and the shock wave associated with the charged particle overcoming of light velocity barrier correspond to infinite jumps of electromagnetic potentials (due to the vanishing of denominators R_i). Thus, they carry a much stronger singularity.

1 Numerical results

We consider the typical case corresponding to $|t| = 2$. The space regions where $D_1 > 0$ and $D_1 < 0$ are shown in fig. 10. There are no physical solutions outside the surface $C_L^{(2)}$.

Accelerated motion.

For the first of the treated problems (uniform acceleration of the charge which initially rests at the origin) all the retarded times t_i and observation time t should be positive (the negative t corresponds to the electrostatic field of the charge at rest). As t_4 is negative (see sect. 4) it should be discarded. The calculations show that the retarded solution t_1 is positive only inside the sphere C_0 of the radius $r = c_n t$ (fig.11). In that region $0 < t_1 < t$. The spherical surface

C_0 corresponds to the bremsstrahlung shock wave originating from the beginning of the charge motion. The points lying inside C_0 describe the radiation from the retarded positions of the charge lying on the positive Z semi-axis. Inside the conic surface $C_M^{(2)}$ lying on the right of $z = 4$ (see fig. 10) the following conditions are satisfied

$$t_3 < 0, \quad t_4 < 0, \quad t_5 > t, \quad t_6 > t, \tag{6.1}$$

which is not acceptable from the physical point of view (as t_5 and t_6 should not exceed the observation time t). The physical region of space where $D_1 > 0$ is bounded by the conic surface $C_M^{(1)}$ and by the surface $C_L^{(1)}$. The Mach cone $C_M^{(1)}$ describes the Čerenkov shock wave, while the surface $C_L^{(1)}$ closing the Mach cone describes the shock wave originating from the charged particle overcoming the light velocity. With a high accuracy the $C_L^{(1)}$ surface is described by the equation $\rho^2 + (z - 1/4)^2 = (t - 1/2)^2$ of the spherical wave emitted from the point $z = 1/4, \quad t = 1/2$ at which the charge velocity coincides with the light velocity in the medium c_n. The region $D_1 > 0$ lying to the left of $z = 4$ consists of two subregions (fig.11). In the first of them lying to the right of C_0 there are two physical solutions t_5 and t_6. The retarded solution t_3 is negative there and, thus, has no physical meaning. In the second subregion lying to the left of C_0 there are three physical solutions $t_3, \quad t_5$ and t_6. The calculations show that the retarded solution t_3 continuously goes into t_1 when one intersects the $D_1 = 0$ surface. The second subregion in turn consists of two subregions corresponding to $q_1 < 0$ and $q_1 > 0$ (fig.12). On the boundary $q_1 = 0$ the following equations are satisfied:

$$t_3(q_1 < 0) = t_6(q_1 > 0), \quad t_5(q_1 < 0) = t_3(q_1 > 0), \quad t_6(q_1 < 0) = t_5(q_1 > 0)$$

The resulting configuration of the shock waves is shown in fig.13. On the internal sides of the surfaces $C_L^{(1)}$ and $C_M^{(1)}$ (where $D_1 > 0$) electromagnetic potentials acquire infinite values (as R_5 and R_6 vanish there). On the external side of $C_M^{(1)}$ lying outside of C_0 the electromagnetic potentials are zero (as there are no solutions there). On the external sides of $C_L^{(1)}$ and of the part of the $C_M^{(1)}$ surface lying inside C_0 the electromagnetic potentials have finite values. With a high accuracy the surface $C_L^{(1)}$ is described by the equation $\rho^2+(z-1/4)^2 = (t-1/2)^2$ of the spherical wave C (shown by short-dash curve in fig.13) emitted from the point $z = 1/4, \quad \rho = 0, \quad t = 1/2$ in which the charge velocity coincides with the light velocity c_n in the medium.

Decelerated motion.

Now we turn to the second problem (uniform deceleration of the charged particle along the positive z semi-axis up to a moment $t = 0$ after which it rests at the origin). In this case only negative retarded times t_i have a physical meaning.

For $t > 0$, in the region where $D_1 < 0$ the retarded time t_2 is everywhere less than zero, while t_1 is negative only outside the circle C_0 (fig.14). In the region where $D_1 > 0$ the retarded solutions t_5 and t_6 are greater than zero and, thus, are not physically admissible. As $t_3 > 0, \quad t_4 < 0$ in the region $D_1 > 0$ bounded by the sphere C_0 and the surface $C_L^{(1)}$, so only t_4 has physical meaning there. It turns out that t_4 continuously passes into t_2 on the surface $C_L^{(1)}$ and on the part of the surface $C_M^{(1)}$ lying inside C_0. In the region $D_1 > 0$ lying outside C_0 both t_3 and t_4 are negative. The calculations show that t_3 and t_4 pass continuously into t_1 and t_2,resp., on the surfaces $C_M^{(1)}$ and $C_M^{(2)}$ lying outside C_0. Thus, surfaces $C_M^{(1)}$ and $C_M^{(2)}$ are pure fictitious for the treated $t > 0, t' < 0$ case. Further, the retarded solutions t_1 and t_2 tend to the same finite values , while the denominators R_1 and R_2 tend to zero when one approaches the internal side of $C_L^{(2)}$ surface (where $D_1 < 0$). The electromagnetic potentials vanish outside of $C_L^{(2)}$ (as no solutions exist there) and acquire infinite values on the internal part of $C_L(2)$ (due to vanishing the denominators R_1 and R_2 there). Therefore, the surface $C_L(2)$ represents the shock wave. The head part of this blunt shock wave with a high accuracy is approximated by the sphere $\rho^2 + (z - 1/4)^2 = (t + 1/2)^2$ (shown by the short-dash curve in fig.14) describing the spherical wave emitted from the point $z = 1/4$ at the moment $t = -1/2$ when the charge velocity coincides with c_n. As a result, for $t > 0, t' < 0$ one has the shock wave $C_L^{(2)}$ and the bremsstrahlung shock wave C_0 arising from the termination of the particle motion. The retarded solution t_2 exists everywhere inside $C_L^{(2)}$, while t_1 exists between C_0 and $C_L^{(2)}$ (fig.14).

Now let the observation time t be less than zero for the decelerated motion. Then all t_i should be less than t. In the region $D_1 < 0$ the retarded solution $t_1 > 0$, which is not physically acceptable. The retarded solution t_2 should satisfy the condition $t_2 < t$. As quantities a and b entering into the definition of t_2 (see Eq.(3.10)) do not depend on the sign of t, the equation $t_2 < t$ is equivalent to

$$-\frac{|t|}{\sqrt{a^2+b^2}} + \frac{1}{\sqrt{2}}(a + \sqrt{a^2+b^2})^{1/2} > |t| \tag{6.2}$$

On the other hand, for the accelerated motion ($t > 0, \quad t_1 > 0$) the condition $t_1 < t$ written in an extended form is

$$-\frac{|t|}{\sqrt{a^2+b^2}} + \frac{1}{\sqrt{2}}(a + \sqrt{a^2+b^2})^{1/2} < |t| \tag{6.3}$$

As (6.3) is satisfied everywhere in the $D_1 < 0$ region, the condition (6.2) cannot be satisfied and the retarded solution t_2 has no physical meaning.

Turning to the region where $D_1 > 0$, one easily obtains from (3.10),(4.1) and (4.7) that the following equations are satisfied:

$$t_4(t<0) = -t_3(t>0), \quad t_3(t<0) = -t_4(t>0), \quad t_5(t<0) = -t_6(t>0),$$

$$t_6(t<0) = -t_5(t>0) \tag{5.5}$$

Consider the solutions t_3 and t_4. Taking into account the negativity of t one may rewrite conditions $t_3 < t$ and $t_4 < t$ in the form $t_3(t < 0) < -|t|, \quad t_4(t < 0) < -|t|$. Or, using (6.4) one gets:

$$t_4(t>0) > |t|, \quad t_3(t>0) > |t| \tag{6.5}$$

. But we have seen earlier that for $t > 0$ the retarded time t_4 is everywhere negative, while t_3 is positive only inside the region bounded by the sphere C_0 and the surfaces $C_L^{(1)}$ and $C_M^{(1)}$ lying inside C_0. In that region t_3 is less than t, which disagrees with (6.5). This in turn means that for $t < 0, t_3 < 0, t_4 < 0$ the conditions $t_3 < t, t_4 < t$ cannot be satisfied and the retarded solutions t_3 and t_4 have no physical meaning.

Further, for $t < 0, t_5 < 0, t_6 < 0$ the conditions $t_5 < t$ and $t_6 < t$ can be rewritten in the form: $|t_5(t<0)| > |t|, \quad |t_6(t<0)| > |t|$. Using (6.4) one gets: $t_5(t > 0) > |t|, \quad t_6(t > 0) > |t|$. But these inequalities are fulfilled only in the part of $D_1 > 0$ region bounded by the $C_M^{(2)}$ surface (see Eq.(5.1) and Fig. 10). As a result, for $t < 0, t' < 0$ the physical solutions t_5 and t_6 exist only inside the Mach cone $C_M^{(2)}$ (fig.15). On its internal boundary (where $D_1 > 0$) the denominators R_5 and R_6 are equal to zero and electromagnetic potentials acquire infinite values. On the external boundary (where $D_1 < 0$) the electromagnetic potentials are zero (as no solutions exist there). Thus, for the case of decelerated motion and the observation time $t = -2$ the only physical solutions are t_5 and t_6 which are contained inside the Mach cone $C_M^{(2)}$ (fig.15).

It remains now to relate the simplified solutions found in sect.5 to the complete solutions found in this section. For the case of accelerated motion the t_1 retarded solution of this section (see fig. 11) on the interval of Z axis $-t < z < t - 1/4$ coincides with the t_1 solution shown

in fig.1; on the part of the Z axis lying between the surfaces $C_L^{(1)}$ and $q_1 = 0$ (Fig. 12) the solutions t_3, t_5, t_6 of fig. 11 coincide with the retarded solutions t_1, t_3, t_2 of fig.1; on the part of Z axis lying to the right of $q_1 = 0$ surface the retarded solutions t_3, t_6, t_5 of fig. 11 coincide with t_3, t_1, t_2 of fig.1.
For the decelerated motion and $t > 0$ the retarded solutions t_1 and t_2 shown in fig.14 on the Z interval $-t < z < t - 1/4$ coincide, respectively, with the t_1 and t_4 solutions presented in fig. 6; the t_4 and t_3 solutions shown in fig. 14 on the part of Z axis lying to the right of $C_L(1)$ surface coincide, respectively, with the t_4 and t_3 solutions (see fig. 6).
For the decelerated motion and $t < 0$ the retarded solutions t_6 and t_5 (see fig.15) on the accessible part of the Z axis $z > t^2$ coincide, respectively, with the simplified solutions t_3 and t_4 shown in fig. 6.

7 Determination of the shock waves positions

So far, we presented the results of numerical calculations. However, a posteriori the boundaries corresponding to the shock waves may be obtained as follows (this method has been extensively used by Schott [5]). We seek the surfaces on which the denominators R_i vanish. The equation $R_i = 0$ may be rewritten in the form:

$$t_i^3 - (z + 1/2)t_i + t/2 = 0 \qquad (7.1)$$

The form of solution depends on the sign of discriminant

$$D = 4(z + 1/2)^3 - \frac{27}{4}t^2$$

For $z < z_c = -1/2 + 3(t/4)^{2/3}$ (in this case $D < 0$) the solution is

$$t_0 = -\frac{1}{4^{1/3}}\{t - [t^2 - \frac{16}{27}(z + 1/2)^3]^{1/2}\}^{1/3} - \frac{1}{4^{1/3}}\{t + [t^2 - \frac{16}{27}(z + 1/2)^3]^{1/2}\}^{1/3} \qquad (7.2)$$

Obviously, $t_0 < 0$ for $t > 0$ and $t_0 > 0$ for $t < 0$. For $z > z_c$ (or $D > 0$) one has

$$t_1 = \mp\frac{2}{\sqrt{3}}\sqrt{z + 1/2}\cos\frac{\phi}{3}, \quad t_2 = \pm\sqrt{z + 1/2}(\frac{1}{\sqrt{3}}\cos\frac{\phi}{3} + \sin\frac{\phi}{3}),$$

$$t_3 = \pm\sqrt{z + 1/2}(\frac{1}{\sqrt{3}}\cos\frac{\phi}{3} - \sin\frac{\phi}{3}) \qquad (7.3)$$

Here $\cos\phi = \frac{\sqrt{27}}{4}|t||z + 1/2|^{-3/2}$, $0 < \phi < \pi/2$. The upper and lower signs in (7.3) correspond to $t > 0$ and $t < 0$, resp. Obviously, $t_1 < 0$, $t_2 > t_3 > 0$ for $t > 0$ and $t_1 > 0$, $t_2 < t_3 < 0$ for $t < 0$.
Combining (7.1) with (4.1) one gets the following equation for ρ^2:

$$\rho_i^2 = t_i^2(z + 1/2) - \frac{3}{2}tt_i + t^2 - z^2 \qquad (7.4)$$

This equation defines the surfaces on which R_i vanish.

Accelerated motion.
Consider the first problem (uniform acceleration along the positive Z semi-axis beginning from the origin at the $t = 0$ moment). Then $t > t_i > 0$. It follows from (7.2) and (7.3) that only t_2 and t_3 have physical meaning. Substituting t_2 and t_3 into (7.4) we easily check that ρ_2 and ρ_3 describe $C_M^{(1)}$ and $C_L^{(1)}$ surfaces. Thus, we obtain the physical picture shown in figs. 16-18 where the positions of Mach cones consisting of the Čerenkov shock waves $C_M^{(1)}$ and of the $C_L^{(1)}$ surfaces closing Mach cones and representing shock waves arising from the charge overcoming of light velocity barrier are presented for different moments of the observation time t. The dimensions of the Mach cones strongly depend on the observation time t. They continuously tend to zero as $t \to 1/2$.

Decelerated motion.
For the case of decelerated motion and the positive observation time ($t > 0$) the physical solutions are t_0 and t_1 (as only they are negative). Substituting them into (7.4) we get ρ_2 and ρ_3 describing the parts of the $C_L^{(2)}$ surface lying on the left and right of the $z = z_c$ plane,resp. For the same decelerated motion and $t < 0$ the physical meaning have t_2 and t_3 (as only they are negative). For the treated case ($t = -2$) the function $\rho^2(t_3) < 0$, which is not accessible. Further, $t_2 > t$ for $z < t^2 = 4$, which is also not permissible (as only $t_i < t$ is allowable). For $z > t^2$ the substitution of t_2 into (7.4) leads to the description of the $C_M^{(2)}$ Mach cone shown in fig. 15. The results of calculations for different times are shown in fig. 19. We see that the sharp Mach cone presented in the right part of this figure ($t = -2, v = 4c_n$) continuously transforms into the blunt shock wave ($t = 2$) shown in the left part of the same figure.

8 Discussion

Consider at first the accelerated motion of the charge beginning from the origin at the moment $t = 0$. All the Mach cones shown in figs. 16-18 exist only for $t > 1/2, z > 1/4$, This means the observer being placed in the space region $z < 1/4$ will not see either Čerenkov shock wave or that of associated with the overcoming of the light velocity barrier. Only the shock wave C_0 (not shown in figs. 16-19) which is due to the beginning of the charge motion reaches him at the moment $t = c_n t$. Moreover, the detection of the aforementioned shock waves ($C_L^{(1)}$ and $C_M(1)$) in the $z > 0$ region is possible if the distance ρ from the Z axis satisfies the equation

$$\rho < \rho_c, \quad \rho_c = \frac{4}{3\sqrt{3}}(z - \frac{1}{4})^{3/2}, \quad z > \frac{1}{4} \qquad (8.1)$$

Inside this region the observer sees at first the Čerenkov shock wave $C_M^{(1)}$. Later he detects the bremsstrahlung shock wave C_0 (not shown in figs.16-19) and the shock wave $C_L^{(1)}$ originating from the overcoming the light velocity barrier. It is remarkable that the surface of the $C_L^{(1)}$ shock wave with a high accuracy coincides with the surface of the sphere $\rho^2 + (z - 1/4)^2 = c_n^2(t - 1/2)^2$ describing the spherical wave emitted by the charge from the point $z = 1/4$ at the moment $t = 1/2$ when the charge velocity is equal to c_n. These spheres are shown by the short-dash curves in figs.16-18. Outside the region defined by (8.1) the observer sees only the bremsstrahlung shock wave C_0 which reaches him at the moment $c_n t = r$.
Further, for $t < 1/2$ only one retarded solution (t_1) exists. It is confined to the surface C_0 of the radius $r = c_n t$. Therefore, the observer will not detect either the Čerenkov shock wave or that of originating from the overcoming of light velocity barrier. The dimensions of the Mach cones shown in figs. 16-18 are zero for $t = 1/2$ and continuously rise with time for $t > 1/2$. The physical reason for this behaviour is that the $C_L^{(1)}$ shock wave closing the Mach cone propagates with the light velocity c_n, while the head part of the Mach cone (i.e., the Čerenkov shock wave $C_M^{(1)}$) attached to the charged particle expands with the velocity $v > c_n$.

In the gasdynamics the existence of at least two shock waves attached to the finite body moving with a supersonic velocity was proved on the very general grounds by Landau and Lifshitz ([10] , Chapter 13). In the present context we associate them with $C_L^{(1)}$ and $C_M^{(1)}$.
For the decelerated motion (see fig.19) the observer in the space region $z < 0$ detects the blunt shock wave $C_L^{(2)}$ first and the bremsstrahlung shock wave C_0 later. It turns out that the head part of this blunt wave with a high accuracy coincides with the sphere $\rho^2+(z-1/4)^2 = (t+1/2)^2$ describing the spherical wave emitted from the point $z = 1/4$ at the moment $t = -1/2$ when the charge velocity coincides with c_n. The observer being placed in the $z > 1/2$ region detects only Čerenkov shock wave $C_M^{(2)}$.

In order not to hamper the exposition, we did not mention, in this section, on the continuous radiation which reaches the observer between the arrival of two shock waves or after the arrival of the last shock wave. It is easily restored either from the simplified case considered in sect. 5 or from figs. 11-15.
However, some precaution is needed. For the motion law (2.4) the charge velocity may exceed c, the velocity of light in vacuum. Consider first the accelerated motion. The external 4-force maintaining the accelerated motion (2.4) becomes infinite (due to the γ-factor ($\gamma = (1-\beta^2)^{-1/2}$) in it). Therefore, this motion cannot be realized for v close to c. In any case, the effects arising from the proximity of charge velocity to c do not produce any discontinuities and will be observed after the arrival of the last of the shock waves considered earlier.
The situation is slightly more complicated for the decelerated motion. To escape the troubles with $v > c$ one may imagine that the charged particle is at rest at the point $z = -z_0$ up to a moment $t = -t_0$, after which it instantly acquires the velocity $c_n < v < c$. After the moment $t = -t_0$ the charge moves towards the origin according a law similar to (2.4). The radiation field arising from such a velocity jump was studied in [9]. It turns out that the arising physical picture insignificantly differs from that considered in previous sections. Let the observation point P lie in the negative Z semi-space. Then, after the arrival of the $C_L^{(2)}$ shock wave, the shock wave C_1 associated with the beginning of the charge motion (at $t = -t_0$) arrives at P. For the observation point P in the positive Z semi-space (more accurately, for $z > 1/4$) the shock wave C_1 reaches P after the arrival of the Čerenkov shock wave $C_M^{(2)}$. In both cases the C_1 shock wave closes either the blunt shock wave $C_L^{(2)}$ or the Mach cone $C_M^{(2)}$ (likewise the shock wave $C_L^{(1)}$ shown in figs.10-14 closes the Mach cone $C_M^{(1)}$). The singularity of the C_1 shock wave is the same as the singularity of C_0 shock wave and, therefore, is weaker than the singularity either of C_M or C_L.

So far we have considered the physical effects arising when the velocity of the point-like charged particle continuously passes through the medium light-velocity barrier. The electromagnetic fields of the uniformly moving charge are well-known both for $v > c_n$ and $v < c_n$ [5,7-9]. But what happens if the particle velocity exactly coincides with the light velocity in the medium c_n ? (This question was posed by Prof. Tyapkin). For this case the equation defining t' is

$$c_n(t-t') = [\rho^2 + (z - c_n t')^2]^{1/2}$$

Solving it relative to t' one gets

$$c_n t' = \frac{1}{2}\frac{r^2 - c_n^2 t^2}{z - c_n t}$$

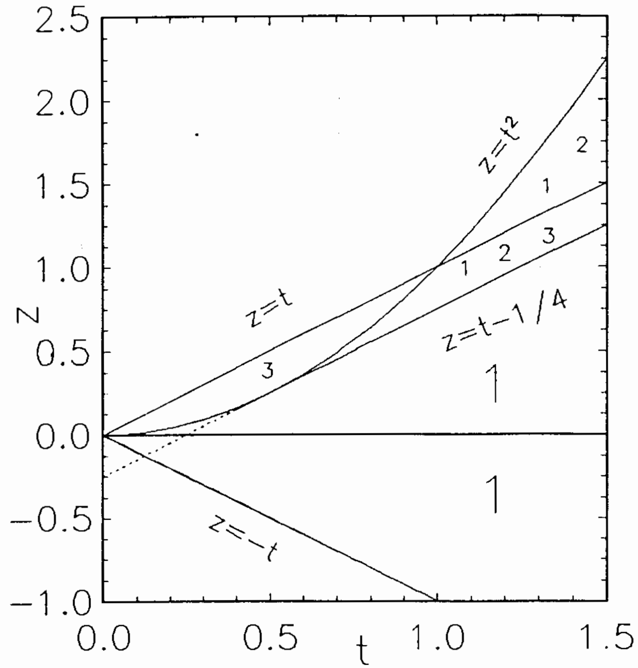

Fig. 1. The space-time distribution of the retarded solutions for the particle in accelerated motion and the observation point lying on the Z axis.

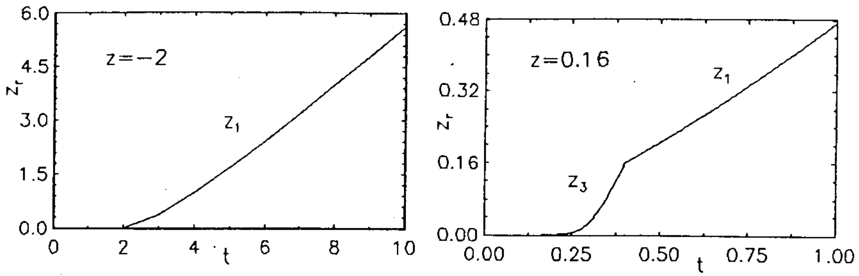

Fig. 2, 3. The retarded positions of the radiating uniformly accelerated charge as functions of time for the observation point lying on the motion axis at $z = -2$ (Fig. 2) and $z = 0.16$ (Fig. 3).

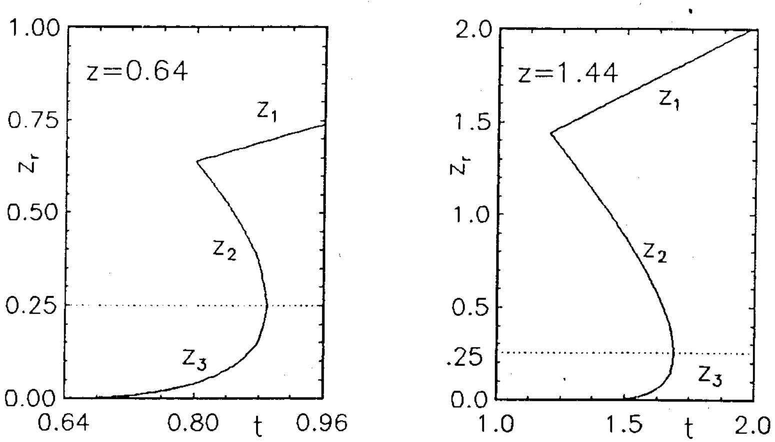

Fig. 4,5. Same as Fig. 2, but for $z = 0.64$ (Fig. 4) and for $z = 1.44$ (Fig. 5).

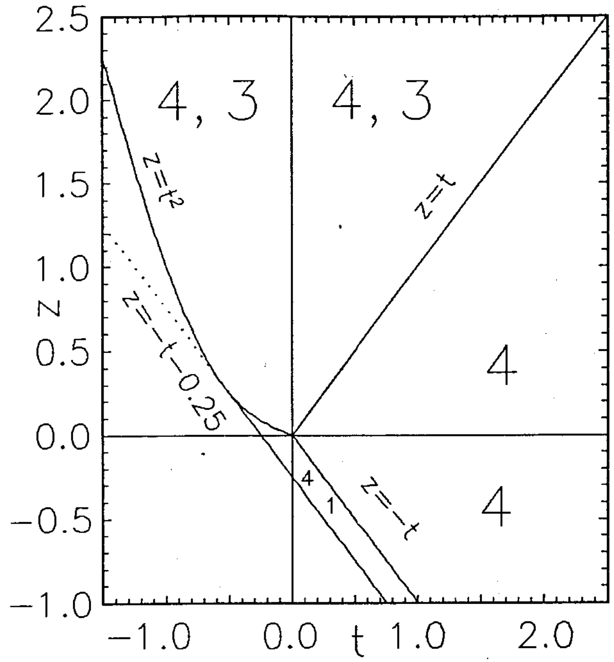

Fig. 6. Same as Fig. 1, but for the decelerated motion.

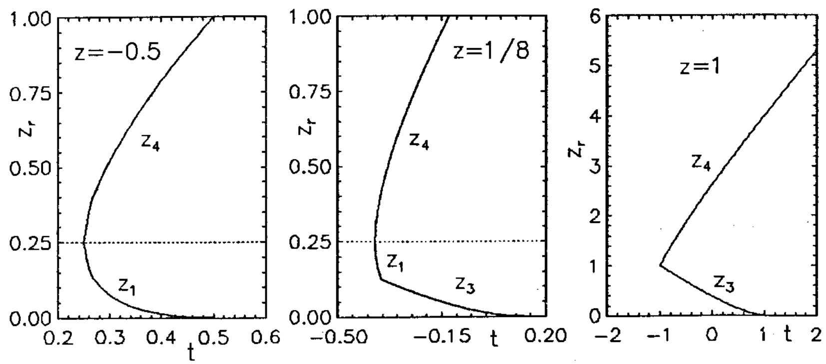

Fig. 7, 8, 9. The retarded positions of the radiating uniformly decelerated charge as functions of time for the observation points on the motion axis at $z = -0.5$ (Fig. 7), $z = 1/8$ (Fig. 8), and $z = 1$ (Fig.9).

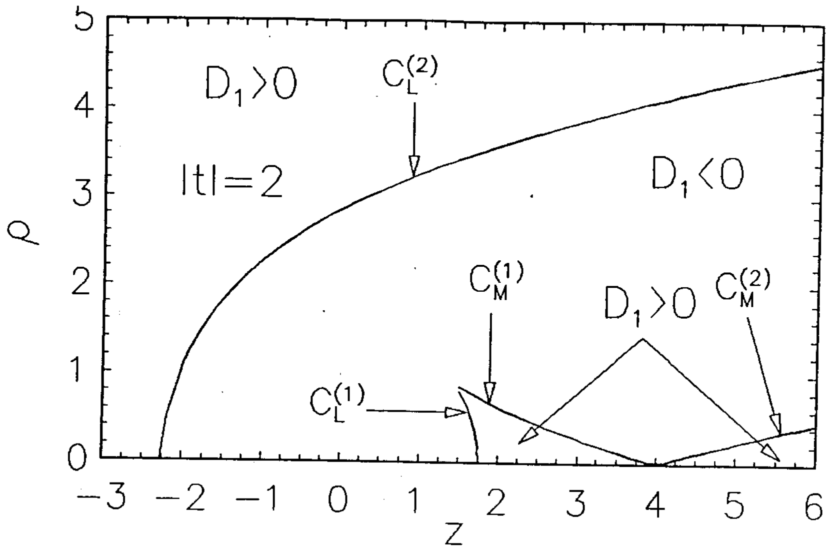

Fig. 10. The space distribution of $D_1 > 0$ and $D_1 < 0$ regions and the shock waves positions for $|t| = 2$.

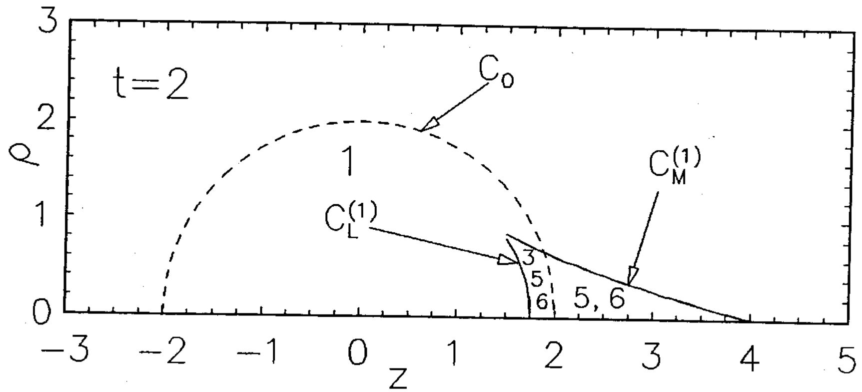

Fig. 11. The space distribution of the retarded solutions and the shock waves positions for the accelerated motion at $t = 2$. Here C_0 denotes the shock wave assosiated with the beginning of the charge motion, $C_M(1)$ denotes the Čerenkov shock wave, $C_L^(1)$ denotes the shock wave originating from the charge overcoming of the light velocity inside the medium.

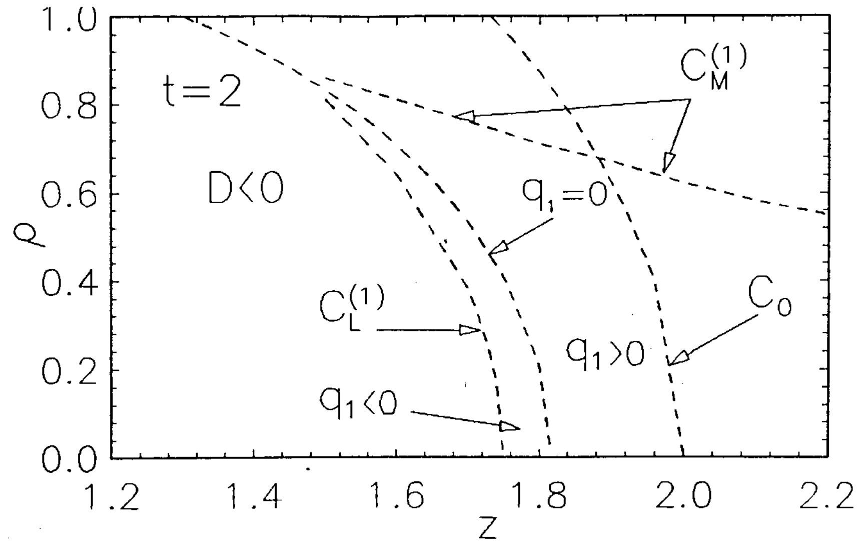

Fig. 12. The magnified representation of Fig. 11.

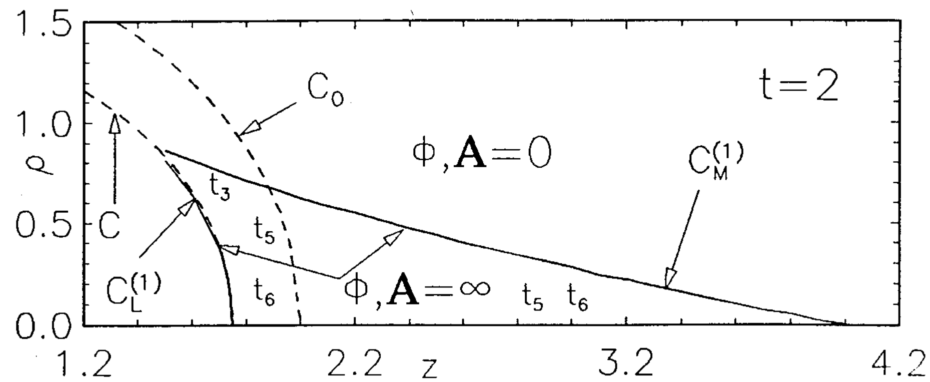

Fig. 13. The distribution of the shock waves for the uniformly accelerated charge for $t = 2$.

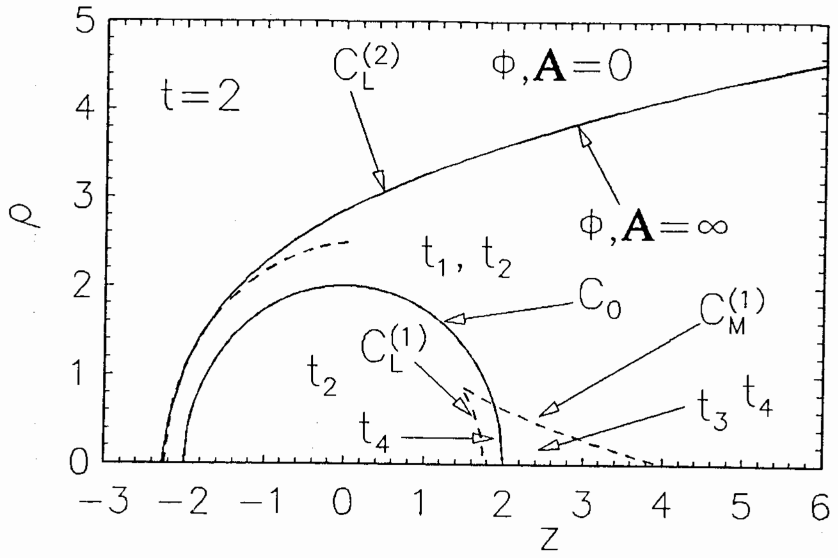

Fig. 14. The distribution of the shock waves for the uniformly decelerated charge for $t = 2$.

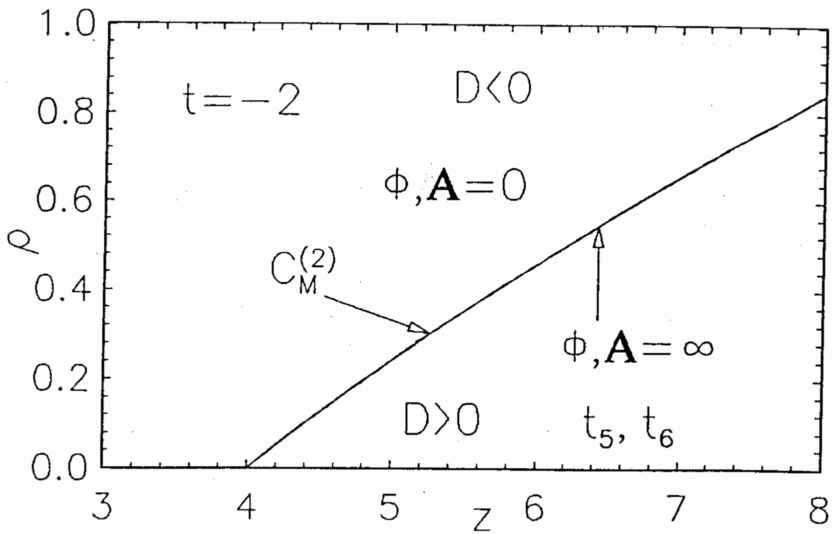

Fig. 15. Same as Fig. 14, but for $t = -2$.

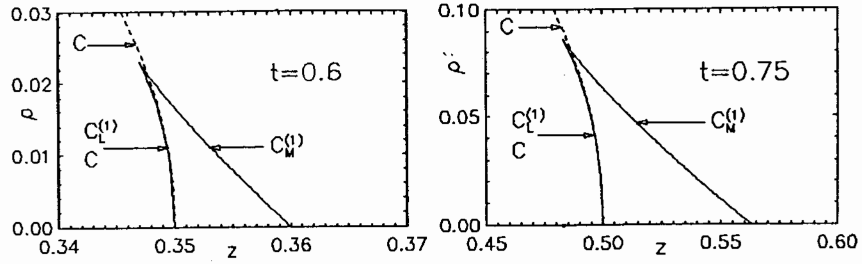

Fig.16,17: The positions of the Čerenkov shock wave $C_M^{(1)}$ and the shock wave $C_L^{(1)}$ arising from the charge overcoming of the light velocity barrier for the accelerated charge are shown for the moment $t = 0.6$ (Fig. 16) and for $t = 0.75$ (Fig. 17). Short dash curve C represents the spherical wave emitted from the point $z = 1/4$ at the moment $t = 1/2$ when the accelerated charged particle overcomes the light velocity barrier.

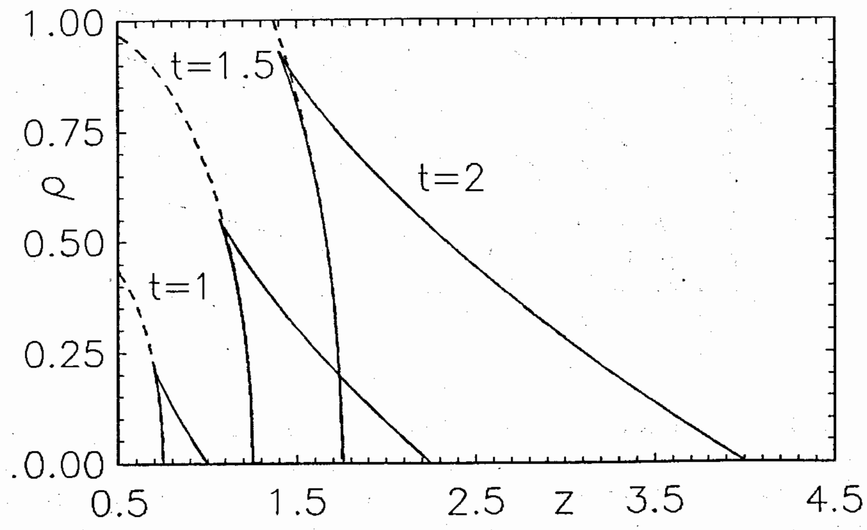

Fig. 18. Same as Fig. 16, but for $t = 1$, 1.5 and $t = 2$.

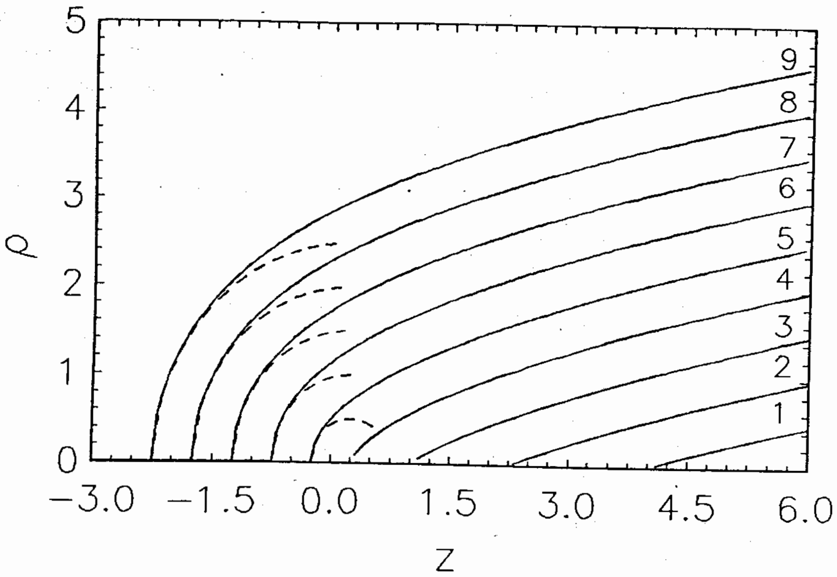

Fig.19: The continuous transformation of the Cerenkov shock wave shown in the right of figure into the blunt shock wave shown in its left part for the decelerated motion. The numbers 1-9 refer to the moments of time $t = -2; -1.5; -1; -0.5; 0; 0.5; 1; 1.5$ and 2, resp. Short-dash curves represent the spherical waves emitted from the point $z = 1/4$ at the moment $t = -1/2$ when the decelerated charged particle overcomes the light velocity barrier.

The nonvanishing components of the electromagnetic potentials are equal to

$$\Phi = \frac{e\Theta(c_n t - z)}{\epsilon(c_n t - z)}, \quad A_z = \frac{ec_n\mu\Theta(c_n t - z)}{c(c_n t - z)}$$

As $\vec{A}$ and Φ do not depend on the cylindrical coordinates ρ and ϕ, so $\vec{B} = \vec{H} = E_\rho = E_\phi = 0$ and

$$E_z = -\frac{\partial\Phi}{\partial z} - \frac{1}{c}\frac{\partial A_z}{\partial t},$$

$$\frac{\partial\Phi}{\partial z} = -\frac{e\delta(c_n t - z)}{\epsilon(c_n t - z)} + \frac{e\Theta(c_n t - z)}{\epsilon(c_n t - z)^2}, \quad \frac{1}{c}\frac{\partial A_z}{\partial t} = \frac{e\delta(c_n t - z)}{\epsilon(c_n t - z)} - \frac{e\Theta(c_n t - z)}{\epsilon(c_n t - z)^2}$$

It turns out that $\vec{E}$ and $\vec{H}$ vanish everywhere except, possibly, the plane $z = c_n t$. In it, E_z reduces to the difference of two infinities and the final answer remains to be undetermined. However, the integral of $\vec{E}$ taken over an arbitrary closed surface surrounding the charge should be equal to $4\pi e$. As $\vec{E}$ is entirely confined to the plane $z = c_n t$, it should be infinite on this plane (to guarantee the finiteness of the above integral). As a result, the electromagnetic field of the particle moving with the velocity coinciding with the light velocity in the medium differs from zero only on the plane normal to the axis of motion and passing through the charge itself. The same ambiguity arises if one takes the explicit formulae describing the charge motion with $v > c_n$ (see e.g., [9]) and will tend $v \to c_n$ in them.
We observe that for $v = c_n$ the shock wave coincides with the $z = c_n t$ plane, i.e., it has an infinite extension. The same effect takes place in gasdynamics when the velocity of the body coincides with the velocity of sound ([10], Chapter 12).

9 Conclusion

Thus, we confirm the qualitative predictions of refs.[2,3] concerning the existence of the shock waves associated with the charge overcoming the light velocity barrier (inside the medium). It would be interesting to observe these shock waves experimentally.

We would like to thank Prof. Tyapkin A.A. for the fruitful discussions and for attraction of our attention to ref. [3].

References

1. I.M. Frank, Vavilov-Čerenkov Radiation. Theoretical Aspects. (Moscow, Nauka, 1988).
2. A.A.Tyapkin, JINR Rapid Communications, No 3, 26-31, (1983).
3. V.P.Zrelov, J.Ruzicka and A.A. Tyapkin, Pre-Čerenkov Radiation as Manifestation of the "Light Barrier", to be published in the Collection of Articles dedicated to P.A. Čerenkov (Nauka, Moscow,1997), in Russian.
4. V.P.Zrelov and J.Ruzicka, Chech. Journal of Physics B, 39 368 (1989);
L.Krupa, J.Ruzicka and V.P.Zrelov, JINR Preprint P2-95-281, Dubna (1995).
5. G.A. Schott, Electromagnetic Radiation (Cambridge, University Press, 1912).
6. B.L. Van der Waerden, Algebra, vol.1. (Springer-Verlag, Berlin, Heidelberg, New York, 1971)
7. O. Heaviside, Electromagnetic Theory, v.3 (London, The Electrician, 1912).
8. A.Sommerfeld, Gotting. Nachricht., 1905, 201.
9. G.N.Afanasiev, Kh.Beshtoev and Yu.P. Stepanovsky, Helv. Phys. Acta, 69, 111 (1996).
10. L.D.Landau and E.M.Lifshitz, Fluid Mechanics (Massachusetts, Addison-Wesley, Reading, 1962).

Received by Publishing Department
on November 14, 1996.